HHS Public Access

Author manuscript

J Invest Dermatol. Author manuscript; available in PMC 2015 November 01.

Published in final edited form as:

J Invest Dermatol. 2015 May ; 135(5): 1415–1424. doi:10.1038/jid.2014.446.

Merkel cell polyomavirus small T antigen is oncogenic in transgenic mice

Monique E. Verhaegen[#1], **Doris Mangelberger**[#1], **Paul W. Harms**[1,3], **Tracy D. Vozheiko**[1], **Jack W. Weick**[1], **Dawn M. Wilbert**[1], **Thomas L. Saunders**[4], **Alexandre N. Ermilov**[1], **Christopher K. Bichakjian**[1], **Timothy M. Johnson**[1,5,6], **Michael J. Imperiale**[7], and **Andrzej A. Dlugosz**[1,8]

[1]Department of Dermatology, University of Michigan, Ann Arbor, MI 48109.

[3]Department of Pathology, University of Michigan, Ann Arbor, MI 48109.

[4]Department of Internal Medicine, University of Michigan, Ann Arbor, MI 48109.

[5]Otolaryngology, University of Michigan, Ann Arbor, MI 48109.

[6]Surgery, University of Michigan, Ann Arbor, MI 48109.

[7]Microbiology and Immunology, University of Michigan, Ann Arbor, MI 48109.

[8]Cell and Developmental Biology, University of Michigan, Ann Arbor, MI 48109.

[#] These authors contributed equally to this work.

Abstract

Merkel cell carcinoma (MCC) is a rare and deadly neuroendocrine skin tumor frequently associated with clonal integration of a polyomavirus, MCPyV, and MCC tumor cells express putative polyomavirus oncoproteins small T antigen (sTAg) and truncated large T antigen (tLTAg). Here, we show robust transforming activity of sTAg *in vivo* in a panel of transgenic mouse models. Epithelia of pre-term sTAg-expressing embryos exhibited hyperplasia, impaired differentiation, increased proliferation and apoptosis, and activation of a DNA damage response. Epithelial transformation did not require sTAg interaction with the PP2A protein complex, a tumor suppressor in some other polyomavirus transformation models, but was strictly dependent on a recently-described sTAg domain that binds Fbxw7, the substrate-binding component of the SCF ubiquitin ligase complex. Postnatal induction of sTAg using a Cre-inducible transgene also led to epithelial transformation with development of lesions resembling squamous cell carcinoma *in situ* and elevated expression of Fbxw7 target proteins. Our data establish that expression of MCPyV sTAg alone is sufficient for rapid neoplastic transformation *in vivo*, implicating sTAg as an oncogenic driver in MCC and perhaps other human malignancies. Moreover, the loss of

Corresponding author: Andrzej A. Dlugosz 3316 Cancer Center, SPC 5932 University of Michigan 1500 E. Medical Center Dr. Ann Arbor, MI 58109-5932 FAX 734 763-4575 Tel 734 647-9482 dlugosza@umich.edu.

CONFLICT OF INTEREST

The authors declare no conflict of interest.

transforming activity following mutation of the sTAg Fbxw7 binding domain identifies this domain as crucial for *in vivo* transformation.

Keywords

Merkel cell polyomavirus; viral oncogenesis; Bowen's disease; T antigen

INTRODUCTION

Merkel cell carcinoma (MCC) is a rare and deadly neuroendocrine malignancy that arises primarily in skin (Bichakjian *et al.*, 2007). While MCC can be cured at early stages, the five year relative survival rate of patients with lymph node involvement is 39%, and a mere 18% for those individuals with distant metastases (Lemos *et al.*, 2010). MCC tumor cells share several markers in common with normal Merkel cells, specialized cells required for transmission of light touch (Maricich *et al.*, 2009) and that arise from progenitors in epidermis (Van *et al.*, 2009; Morrison*et al.*, 2009). However, the cell of origin of MCC is not known (Tilling and Moll, 2012).

The lack of effective treatments for advanced MCC has fueled studies into the molecular basis of MCC with the hope of identifying new targets for therapy. A pivotal report by Moore and coworkers identified a novel polyomavirus, named Merkel cell polyomavirus (MCPyV), in 8 of 10 human MCC samples by digital transcriptome subtraction (Feng *et al.*, 2008). Subsequent studies confirmed these findings, with approximately 75% of MCCs harboring MCPyV sequence [reviewed in (Jaeger *et al.*, 2012)]. Polyomaviruses are double-stranded DNA viruses that include murine polyomavirus, simian virus 40, and at least 12 human polyomaviruses, including MCPyV and several other polyomaviruses identified specifically in skin (DeCaprio and Garcea, 2013). Although several polyomaviruses have been implicated in human cancer development (Zur Hausen, 2008), compelling evidence supporting this concept is limited to MCPyV, making this virus a crucial focus for investigation.

MCPyV DNA in MCCs is integrated clonally (Feng *et al.*, 2008), strongly suggesting that this virus is present at tumor initiation and that one or more viral proteins function as oncogenic drivers. Like that of other polyomaviruses, the MCPyV genome contains an early region with genes encoding the putative transforming antigens large T (LTAg) and small T (sTAg) and a late region with genes encoding the viral capsid components (DeCaprio and Garcea, 2013). MCPyV-positive tumor cells express sTAg and LTAg with tumor-specific C-terminal truncations (tLTAg) which disrupt viral helicase activity but retain the consensus domain for binding to the retinoblastoma 1 (RB1) tumor suppressor protein (Shuda *et al.*, 2008). TAgs from other polyomaviruses contribute to transformation and tumorigenesis by interacting with key cellular factors: most LTAgs disrupt the function of RB1 and TP53 tumor suppressors while sTAgs inhibit the PP2A tumor suppressor complex (DeCaprio and Garcea, 2013; Dalianis and Hirsch, 2013). In general, LTAg is the dominant transforming oncogene for most polyomaviruses and sTAg either does not transform or does so with low efficiency, but cooperates to mediate the full transformation potential of LTAg [reviewed in

(Khalili *et al.*, 2008)]. It was recently reported that MCPyV encodes a third early protein called ALTO whose role in transformation, if any, is not yet known (Carter *et al.*, 2013).

MCPyV sequences have been detected in various tumor types other than MCC, but the significance of these findings is unclear in light of the widespread prevalence of this virus in the general population, the generally low virus copy number in non-MCC tumors, and detection of MCPyV sequences in normal tissues as well as cancer tissues. Interestingly, a small number of MCPyV-positive cases of chronic lymphocytic leukemia (CLL) and non-small cell lung cancer (NSCLC) harbor tumor-specific LTAg mutations and express LTAg protein (Pantulu *et al.*, 2010; Hashida *et al.*, 2013). In addition, viral integration was demonstrated in NSCLC (Hashida*et al.*, 2013), in keeping with a functional role for MCPyV in the development of tumors other than MCC.

Genetic knock-down of tLTAg and sTAg, or either tLTAg or sTAg alone, leads to reduced proliferation of MCC cell lines and/or tumor xenografts, arguing that TAg expression is required for maintenance of cultured MCC tumor cells (Houben *et al.*, 2010; Shuda *et al.*, 2014). In other studies, however, knock-down of either tLTAg (Houben *et al.*, 2012) or sTAg (Angermeyer *et al.*, 2013) had no effect on tumor cell proliferation or viability *in vitro*, raising the possibility that in some cases, MCPyV may lead to tumor development through a hit-and-run mechanism [reviewed in (Niller *et al.*, 2011)]. In contrast to TAgs from other polyomaviruses, *in vitro* studies revealed that MCPyV sTAg, and not LTAg, is capable of driving a transformed phenotype in rodent fibroblasts (Shuda *et al.*, 2011; Kwun *et al.*, 2013). This is not dependent on sTAg interaction with PP2A (Shuda *et al.*, 2011), but does require a domain that binds SCF^{Fbxw7} and leads to accumulation of several cellular oncoproteins and LTAg, designated the LT-stabilization domain (LSD) (Kwun *et al.*, 2013).

Cell culture studies (Shuda *et al.*, 2011; Kwun *et al.*, 2013) have set the stage for *in vivo* analysis of MCPyV TAg transforming potential, which we have now examined using a panel of transgenic mice carrying wild-type or mutant sTAgs. We show that expression of sTAg in pre-term embryos is sufficient for transformation of several epithelia including skin. The phenotypes are independent of PP2A-binding but strictly dependent on the recently described sTAg LSD. In adult mice, sTAg drives rapid epidermal hyperplasia and development of skin lesions resembling SCC *in situ*. Our findings identify sTAg as a powerful oncogenic driver *in vivo*, support the concept that MCPyV may play a role in the development of tumors other than MCC, and establish a strict requirement for the sTAg LSD for epithelial transformation in mice.

RESULTS

Epithelial transformation in transgenic mouse embryos expressing MCPyV sTAg

We used a transgenic cassette with 5.3 kb bovine K5 promoter (Ramirez *et al.*, 1994) to target expression of sTAg to epidermis and several other epithelia. We constructed the *K5-sTAg* transgene with an internal ribosomal entry site (IRES) and tdTomato cDNA downstream of sTAg, enabling us to use immunostaining for RFP (tdTomato) as an indicator of transgene expression (Figure 1A, Table S1). Since we could not predict the biological response of K5-targeted cells to sTAg expression, we analyzed pre-term

transgenic embryos to circumvent a potentially severe phenotype incompatible with postnatal survival. Histology of *K5-sTAg* embryos revealed striking alterations in several epithelia where the K5 promoter was active, including skin, tongue, palate, tooth primordia, and salivary glands (Figure 1B, Table S1). The most severe changes were detected in acral skin and oral cavity, and typically included the replacement of differentiated epithelial cell layers by an expanded and disorganized epithelium (Figure 1B). Mitotic cells, largely restricted to the basal and first suprabasal layer in control epithelia, were detected in mid and upper cell layers in *K5-sTAg* mice, and condensed or fragmented nuclei suggestive of apoptosis were frequently observed, typically limited to the uppermost strata of affected epithelia (Figure 1B). Similar changes were seen in multiple independent transgenic founders (Table S1).

MCPyV sTAg drives alterations in epithelial differentiation, proliferation, and apoptosis

Immunostaining for RFP showed a strong correlation between transgene expression and epithelial abnormalities. RFP was not detected or was only present in a small number of cells in *K5-sTAg* mice that lacked any apparent phenotypic changes (Table S1). In contrast, in embryos with dysplastic epithelia, RFP was frequently expressed throughout multiple cell layers (Figure 2A). Analysis of epithelial lineage markers revealed an altered program of terminal differentiation. Cells expressing keratin K5, normally limited to the basal and lower suprabasal cell layers, were detected in suprabasal strata of epidermis and tongue in *K5-sTAg* mice (Figure 2B). In contrast, the number of cell layers expressing the late-stage epidermal differentiation marker loricrin was reduced (Figure 2B). In some areas, the outermost cellular compartment in epidermis, the stratum corneum, was also reduced in thickness (Figure 1B, 2A).

There was a marked expansion of cells expressing the proliferation markers Ki67 and pHH3 in affected epithelia (Figure 2C) and many cells expressed the apoptosis marker cleaved caspase 3 (CC3), particularly in upper strata (Figure 2D). Expression of γH2AX, an indicator of DNA damage frequently detected in cancer (Bonner *et al.*, 2008), was also elevated in epithelia of *K5-sTAg* mice (Figure 2D). In mosaic founders (Table S1), the above alterations were largely limited to RFP-expressing cells, indicating that these epidermal responses to sTAg are largely cell-autonomous. Collectively, these data establish that expression of MCPyV sTAg *in vivo* is sufficient to produce multiple phenotypic alterations that are associated with epithelial neoplasia.

In vivo transformation by MCPyV sTAg is not dependent on interaction with PP2A

To begin testing for a potential mechanism regulating sTAg's potent transforming activity *in vivo* we first focused on the PP2A tumor suppressor complex (Westermarck and Hahn, 2008; Mumby, 2007), which is targeted by sTAgs from other polyomaviruses to alter mammalian cell function (Sablina and Hahn, 2008; Andrabi *et al.*, 2011; Rodriguez-Viciana *et al.*, 2006). We modified the *K5-sTAg* cassette to yield a mutant sTAg carrying a leucine to alanine substitution at amino acid 142 (sTAgL142A) (Figure 3A), which disrupts interaction with both the Aα structural subunit and catalytic C subunit of PP2A (Shuda *et al.*, 2011). The phenotype of *K5-sTAgL142A* mice was similar to that of *K5-sTAg* mice (Figure 3B, Figure S1A, Table S1) and included impaired differentiation, an expanded proliferative

compartment and nuclear fragmentation (Figs. 3B). Immunostaining revealed an increased proportion of Ki67-expressing cells, impaired differentiation, increased apoptosis, and expression of γH2AX (Figure S1A). These data argue that binding of sTAg to the PP2A tumor suppressor is not required for *in vivo* transformation in epithelia.

In vivo transformation by sTAg is strictly dependent on the LTAg stabilization domain (LSD)

In contrast to the PP2A binding domain, the sTAg LSD is essential for transformation in cultured cells. Mutant sTAg with alanine substitutions at amino acids 91-95, which no longer co-immunoprecipitates with overexpressed Fbxw7 (Kwun *et al.*, 2013), prevents accumulation of LTAg and several cellular targets, and fails to transform fibroblasts. To test the *in vivo* transforming potential of this LSD mutant, we generated a *K5-sTAg91-95A* transgenic construct (Figure 4A) and produced additional transgenic embryos. Strikingly, histology of epidermis from *K5-sTAg91-95A* pre-term embryos was indistinguishable from that of controls (Figure 4B), and immunostaining to detect a panel of epidermal markers, Ki67, CC3, and γH2AX supported this impression (Figure 4C). RFP expression confirmed robust transgene expression in epidermal basal cells where the K5 promoter is active under normal conditions (Figure 4B). Thus, in striking contrast to the robust *in vivo* transforming potential of wild-type or PP2A binding-deficient sTAg, the sTAg LSD mutant fails to drive epithelial transformation in pre-term embryos.

Postnatal activation of MCPyV sTAg leads to epidermal transformation and squamous cell carcinoma *in situ*

To assess the transforming potential of sTAg in adult mice, we engineered Cre-inducible sTAg transgenic mice, designated *KLEsT*, using a modified K5 construct (Allen *et al.*, 2003) which contains a floxed enhanced GFP/STOP sequence upstream of the sTAg cDNA (Figure 5A). *KLEsT* mice express GFP in K5-expressing cells, but in the presence of Cre, recombination at the loxP sites leads to deletion of the GFP/STOP sequence and transcription of the previously dormant sTAg cDNA (Figure 5A). We crossed *KLEsT* mice with *K5-CreERT2* mice (Indra *et al.*, 1999) carrying a tamoxifen-inducible Cre to generate *K5-CreERT2;KLEsT* (*iK5;KLEsT*) bitransgenic mice. Treatment of these mice with tamoxifen to activate sTAg expression led to profound alterations in epidermis at several body sites including tail, ear, snout, and volar skin (Figure 5B,C). Affected epidermis was markedly hyperplastic, with the most striking changes in ear epidermis which was over 10-fold thicker than in control mice ($P<0.001$) (Figure 5D). Cells with condensed or fragmented nuclei were common and epidermal maturation was altered in some areas, with absence of a granular cell layer, abrupt keratinization, and regions of prominently thickened stratum corneum containing retained nuclei (parakeratosis) (Figure 5B). In some areas, the histological changes were more advanced and included full-thickness atypia, reduced eosin staining, pycnotic nuclei, and tissue disorganization, which collectively recapitulate many features of human SCC *in situ* (Bowen's disease) (Figure 5E). We detected sTAg in *iK5-KLEsT* mice exhibiting a strong epidermal phenotype using immunoprecipation followed by immunoblotting of skin lysates with the 2t2 monoclonal antibody (Schwitalla *et al.*, 2013) (Figure 5F) which recognizes MCPyV TAgs (Shuda *et al.*, 2014).

Immunostaining of skin from adult sTAg-expressing mice revealed expansion of Ki67-expressing cells and an increased number of cells expressing CC3 and γH2AX (Figure 6A), reflecting changes we detected in pre-term *K5-sTAg* embryos. Immunostaining for lineage markers again revealed an expanded population of cells expressing K5 and the appearance of hyperplasia-associated keratins K6 and K17 (Figure 6B,C). Occasionally, expression of the granular cell marker loricrin and spinous cell marker K10 was focally reduced or absent beneath regions of parakeratosis (Figure 6B). Although K20, K8, and synaptophysin were easily detected in normal Merkel cells, these markers were not appreciably induced in hyperplastic regions of epidermis from *iK5-KLEsT* mice (Figure S2). Postnatal activation of sTAg in cutaneous epithelia thus mimics many of the changes seen in transgenic embryos, and in some areas leads to lesions closely resembling human SCC *in situ*, but expression of sTAg alone does not appear to be sufficient to drive epidermal cells into the Merkel cell lineage.

In vivo transformation by sTAg is associated with accumulation of Fbxw7 targets

The sTAg LSD is required for fibroblast transformation *in vitro* (Kwun *et al.*, 2013) and epithelial transformation *in vivo* (Figure 4), and is proposed to function at least in part by stabilizing LTAg and cellular proteins targeted for destruction by the SCF/Fbxw7 ubiquitin ligase complex (Kwun *et al.*, 2013). We therefore performed immunoblotting to assess whether epidermal transformation in adult mice was associated with accumulation of Fbxw7 targets. Expression levels of cyclin E, c-Jun, mTOR, and Mcl-1, all of which are Fbxw7 substrates targeted for destruction by the SCF complex (Koepp *et al.*, 2001; Nateri *et al.*, 2004; Mao *et al.*, 2008; Inuzuka *et al.*, 2011), were elevated in skin lysates of *iK5;KLEsT* mice relative to controls (Figure 6D). Increased expression of PCNA and K17 confirmed a hyperplastic response and loss of GFP indicated efficient recombination of the KLEsT transgene. These data are in keeping with the idea that binding of sTAg to Fbxw7 impairs its ability to target key cellular proteins for ubiquitin-mediated degradation, leading to their accumulation and potential contribution to sTAg-driven transformation.

DISCUSSION

The discovery of clonally integrated MCPyV viral sequences in the majority of human MCCs argues that MCPyV TAgs play a causal role in tumor development. We now present studies examining the tumorigenic potential of sTAg when expressed *in vivo* in pre-term transgenic mouse embryos and adult mice. sTAg expression can promote neoplastic transformation in epithelia of late-stage mouse embryos in a PP2A-independent and sTAg LSD-dependent manner, while activation of sTAg in skin of adult mice leads to similar transformation-related changes and also drives the development of lesions resembling SCC *in situ*. These findings establish sTAg as a potent oncogene *in vivo*, and suggest that it functions as an oncogenic driver in MCC and potentially other cancers linked to MCPyV. The strict requirement for the Fbxw7-binding LSD region in epithelial transformation of pre-term embryos, coupled with the upregulation of multiple oncogenic Fbxw7 targets in adult mice expressing sTAg, suggest that sTAg-Fbxw7 binding and stabilization of key cellular substrates may contribute to sTAg-driven epithelial transformation *in vivo*.

Epithelial abnormalities in pre-term *K5-sTAg* embryos exhibit features in common with many neoplasms, including altered differentiation, an expanded proliferative compartment, increased apoptosis, and a robust DNA damage response. To delineate the potential mechanism by which sTAg drives these profound alterations in cell and tissue function, we analyzed the response to sTAg mutants defective in binding to either the tumor suppressor PP2A (sTAgL142A) or Fbxw7 (sTAg91-95A), the substrate-binding component of the SCF ubiquitin ligase complex which has tumor suppressor activity in a broad range of malignancies [reviewed in (Cheng and Li, 2012)]. We found that the PP2A binding site of sTAg is not required for epithelial transformation in pre-term embryos, in keeping with results obtained using cultured fibroblasts (Shuda *et al.*, 2011; Kwun *et al.*, 2013). In contrast, transforming activity is lost in mice carrying the sTAg91-95A LSD mutant which no longer binds Fbxw7 (Kwun *et al.*, 2013); moreover, the expression of several Fbwx7 substrates is elevated in skin of adult mice expressing wild-type sTAg. These data suggest that sTAg drives transformation *in vivo*, at least in part, via up-regulation of cellular proteins targeted for destruction by the SCF/Fbxw7 complex. However, it is unlikely that the loss of transforming potential of the sTAg91-95A LSD mutant is due solely to disruption of normal Fbwx7 function, since Fbwx7 knockdown failed to fully restore fibroblast transformation by the sTAg91-95A LSD mutant (Kwun *et al.*, 2013). Further studies will be required to define additional functions of the sTAg91-95A LSD mutant which may contribute to, or play a central role in, transformation.

The development of SCC in situ in adult mice expressing sTAg raises the possibility that MCPyV plays a role in the development of other skin tumors or perhaps extracutaneous malignancies. In keeping with this possibility, MCPyV sequences have been detected in a few cases of CLL and NSCLC which harbor tumor-specific LTAg truncations and express tLTAg protein (Pantulu *et al.*, 2010; Hashida *et al.*, 2013). Of potential relevance to our findings in adult mice, one study documented MCPyV mutations that would yield tumor-specific LTAg truncation in human SCCs (Dworkin *et al.*, 2009), although viral integration and copy number were not examined. Unfortunately, immunoreagents to selectively detect MCPyV sTAg are not readily available, so with the exception of a single report (Shuda *et al.*, 2011), immunostaining for TAg protein expression in MCPyV-positive tumors has been limited to LTAg or tLTAg.

Although the striking phenotypes seen in embryos and adult sTAg-expressing mice establish the transforming potential of sTAg expressed in epithelial cells, we did not detect lesions resembling MCC either morphologically or biochemically by immunostaining for a panel of MCC markers. Expression of sTAg alone in K5-expressing epidermal cells is thus not sufficient to drive MCC development in the context of this type of mouse model. This raises questions about the potential requirement for tLTAg and/or additional somatic mutations in MCC pathogenesis. Since both sTAg and tLTAg appear to be coexpressed in most MCPyV-positive MCCs and tLTAg is required for MCC tumor cell maintenance, it seems likely that tLTAg plays an important role in MCC tumorigenesis. Tumor-specific LTAg truncations are always downstream of the domain that binds the tumor suppressor RB1, which may be a critical cellular target for MCPyV as it is in human papillomavirus-associated cancer. In keeping with this concept, MCCs that are MCPyV-negative have either lost or reduced

endogenous RB1 expression (Sihto *et al.*, 2011; Harms *et al.*, 2013), and in some cases this is associated with somatic mutations leading to premature termination codons (Cimino *et al.*, 2014).

The absence of MCCs in sTAg-expressing mice may also be related to the fact that our modeling strategy does not target transgene expression to a cell population competent to give rise to MCC. The potential cell of origin of MCC is controversial, and may include epidermal cells, Merkel cell progenitors residing in the epidermis, or even differentiated Merkel cells. Expression of the epithelial marker p63 in MCC (Asioli *et al.*, 2007; Hall *et al.*, 2012; Stetsenko *et al.*, 2013) is in keeping with the idea that at least some MCCs are derived from epidermal basal cells or Merkel cell progenitors which co-express epidermal and Merkel cell markers. Additional modeling studies, testing the tumorigenic potential of sTAg alone or combined with tLTAg, will be required to assess whether expression of MCPyV TAgs in appropriate progenitor cells is sufficient to drive MCC development in mice.

In summary, we have utilized a powerful transgenic mouse embryo screening assay, coupled with Cre-inducible mouse lines for postnatal transgene induction, to establish that MCPyV sTAg has robust transforming activity *in vivo*. Our data suggest that sTAg functions as an oncogenic driver in MCC and perhaps other MCPyV-associated human tumors, and may provide an important target for drug development. Future studies will focus on identifying the mechanism by which sTAg drives transformed phenotypes *in vivo*, and ascertaining whether combined expression of MCPyV sTAg and tLTAg in defined cell populations in skin can give rise to murine tumors resembling human MCCs.

MATERIALS AND METHODS

Generation of transgenic mice

The *K5-sTAg-IRES-tdTomato* (*K5-sTAg*) transgenic cassette was generated as follows: a sTAg cDNA sequence (GenBank EU375803; nts 196;756) including an additional upstream Kozak sequence, a 5′ NotI site and a 3′ SnaBI site was synthesized de novo by GenScript USA (Piscataway, NJ) and cloned into the pUC57 vector. A NotI-sTAg-SnaBI digested fragment was then sub-cloned into the pBK5 vector (Ramirez *et al.*, 1994) containing an *IRES-tdTomato* sequence synthesized and subcloned by GenScript USA based on the pLVX-IRES-tdTomato vector (Clontech, cat# 631238; nts 2842-4847). Site directed mutagenesis using the GENEART Site-Directed Mutagenesis System (Life Technologies, NY) was used to create a leucine to alanine substitution at amino acid 142 to generate the *K5-sTAgL142A* cassette. The *K5-sTAg91-95A* cassette was generated with a nucleotide sequence substituting amino acid residues 91-95 with alanines (Kwun *et al.*, 2013) by GenScript USA using site directed mutagenesis. Following sequence verification, BssHII-digested fragments of each of the above constructs were purified and injected into (C57BL/6 X SJL) F2 mouse eggs in the University of Michigan Transgenic Core. The inducible *K5-loxP-eGFP-loxP-sTAg* (*KLEsT*) transgenic cassette was subcloned by GenScript USA using the pUC57-sTAg vector described above into a SnaBI-blunt restriction digested *K5-loxP-eGFP-loxP* (Allen *et al.*, 2003) vector backbone.

Analysis of pre-term embryos

To avoid loss of transgenic founders with lethal phenotypes, pre-term embryos from all conventional K5 driven transgenic mice were harvested at e18.5 and founders identified by PCR using transgene-specific primers as described in Supplementary Material. The number of transgene-positive/ total potential embryonic founders was as follows: K5-sTAg: 11/92, K5-sTAgL142A: 5/18, and K5-sTAg91-95A: 11/122. Detailed analysis of sTAg embryo harvests is provided in Table S1.

Postnatal transgene induction

KLEsT mice were crossed with *K5-CreERT2* (Indra *et al.*, 1999) mice (kindly provided by Drs. Pierre Chambon and Daniel Metzger) to generate *K5-CreERT2;KLEsT* (*iK5;KLEsT*) bitransgenic mice for analysis. Recombination leading to sTAg expression was induced in P21 mice by 5 daily oral gavage administrations of 75mg/kg tamoxifen (Sigma-Aldrich) resuspended in corn oil. KLEsT founder mice were crossed with C57BL/6J breeders (Jackson Laboratory, ME) to establish transgenic lines. All mice were housed and maintained according to University of Michigan institutional guidelines. Procedures involving animal experimentation were approved by the University Committee on the Use and Care of Animals, animal protocol #PRO00004440.

Tissue collection and immunostaining

All tissues were fixed overnight at room temperature in 10% neutral buffered formalin, transferred to 70% EtOH, processed, and paraffin embedded. For immunohistochemical staining, tissue was sectioned at 5μM, deparaffinized and rehydrated prior to antigen retrieval in boiling citrate-based buffer (0.01 mol/L citric acid, pH 6.8). Endogenous peroxidases were quenched with 3% H_2O_2, followed by blocking in 5% goat serum and incubation with primary antibodies (see Supplementary Material for details). Bound antibodies were detected with the Vector M.O.M. peroxidase or fluorescein Immunodetection Kits (Vector Laboratories, CA), using SigmaFast diaminobenzidene as a peroxidase substrate or AlexaFluor594 (Jackson ImmunoResearch, PA) for immunofluorescence. Nuclei were counterstained with hematoxylin followed by Permount (Fisher Scientific) mounting or immunofluorescence visualized with ProLong Gold Antifade Reagent with DAPI (Invitrogen, OR).

Immunoblotting and immunoprecipitation

Epidermal lysates were prepared by mechanical homogenization in RIPA buffer supplemented with HALT phosphatase inhibitor cocktail (Thermo Scientific, IL) and Complete mini protease inhibitor cocktail (Roche, IN) followed by protein quantification using standard Bradford method with Bio-Rad Protein Assay dye reagent (Bio-Rad Laboratories, CA). For immunoprecipitation, 500 μg of pre-cleared protein lysate was incubated with 5 μg of primary mouse 2t2 antibody overnight at 4°C followed by binding to Protein G Sepharose beads (GE Healthcare, Sweden). Beads were centrifuged, washed, and the pellet dissolved in Laemmli buffer. Supernatants were separated on 4-20% or 12% gradient SDS-polyacrylamide gels followed by transfer to Immobilon-P membranes (Millipore, MA). Antibody details are listed in Supplementary Material. Detection was

carried out with SuperSignal West Pico or Femto chemiluminescent substrates (Thermo Scientific, IL).

Quantification of epidermal thickness

Epidermal thickness at each site (tail, ear, volar, snout) was measured as an average from 4 fields in 3 independent mice. Statistics were performed using an unpaired two-tailed Student's t test.

Supplementary Material

Refer to Web version on PubMed Central for supplementary material.

ACKNOWLEDGEMENTS

We thank Joanna Pero, Natalia Loaiza, and Ehab Nazzal for additional technical assistance, Eric Fearon for insightful comments on the manuscript, and Chris Buck, Pierre Coulombe, Daniel Metzger, Pierre Chambon, and José Jorcano for providing mice and/or reagents. We gratefully acknowledge Wanda Filipiak and Galina Gavrilina of the Transgenic Animal Model Core of the University of Michigan's Biomedical Research Core Facilities for production of transgenic mice. This work was supported by a Research Career Development Award (MEV), Dermatopathology Research Career Development Award (PWH), and Clinical Career Development Award in Dermatologic Surgery (CKB), each from the Dermatology Foundation; the Helen L. Kay Charitable Trust; the Ronald P. and Joan M. Nordgren Cancer Research Funds (AAD); and the National Institutes of Health, through the University of Michigan's Cancer Center Support Grant (CA046592), the University of Michigan Gastrointestinal Peptide Research Center Grant (DK34933), and R01s CA087837, AR045973, and R21 CA183084 (AAD).

Abbreviations

MCC	Merkel cell carcinoma
MCPyV	Merkel cell polyomavirus
sTAg	small T antigen
LTAg	large T antigen
tLTAg	truncated large T antigen
LSD	large T stabilization domain
PP2A	protein phosphatase 2A
K5	keratin 5
RFP	red fluorescent protein
SCC	squamous cell carcinoma

REFERENCES

Allen M, Grachtchouk M, Sheng H, et al. Hedgehog signaling regulates sebaceous gland development. Am J Pathol. 2003; 163:2173–2178. [PubMed: 14633591]

Andrabi S, Hwang JH, Choe JK, et al. Comparisons between murine polyomavirus and Simian virus 40 show significant differences in small T antigen function. J Virol. 2011; 85:10649–10658. [PubMed: 21835797]

Angermeyer S, Hesbacher S, Becker JC, et al. Merkel cell polyomavirus positive Merkel cell carcinoma cells do not require expression of the viral small T antigen. J Invest Dermatol. 2013; 133:2059–2064. [PubMed: 23439392]

Asioli S, Righi A, Volante M, et al. p63 expression as a new prognostic marker in Merkel cell carcinoma. Cancer. 2007; 110:640–647. [PubMed: 17599745]

Bichakjian CK, Lowe L, Lao CD, et al. Merkel cell carcinoma: critical review with guidelines for multidisciplinary management. Cancer. 2007; 110:1–12. [PubMed: 17520670]

Bonner WM, Redon CE, Dickey JS, et al. GammaH2AX and cancer. Nat Rev Cancer. 2008; 8:957–967. [PubMed: 19005492]

Carter JJ, Daugherty MD, Qi X, et al. Identification of an overprinting gene in Merkel cell polyomavirus provides evolutionary insight into the birth of viral genes. Proc Natl Acad Sci U S A. 2013; 110:12744–12749. [PubMed: 23847207]

Cheng Y, Li G. Role of the ubiquitin ligase Fbw7 in cancer progression. Cancer Metastasis Rev. 2012; 31:75–87. [PubMed: 22124735]

Cimino PJ, Robirds DH, Tripp SR, et al. Retinoblastoma gene mutations detected by whole exome sequencing of Merkel cell carcinoma. Mod Pathol. 2014 E-pub:1-15.

Dalianis T, Hirsch HH. Human polyomaviruses in disease and cancer. Virology. 2013; 437:63–72. [PubMed: 23357733]

DeCaprio JA, Garcea RL. A cornucopia of human polyomaviruses. Nat Rev Microbiol. 2013; 11:264–276. [PubMed: 23474680]

Dworkin AM, Tsengf SY, Allain DC, et al. Merkel cell polyomavirus in cutaneous squamous cell carcinoma of immunocompetent individuals. J Invest Dermatol. 2009; 129:2868–2874. [PubMed: 19554019]

Feng H, Shuda M, Chang Y, et al. Clonal integration of a polyomavirus in human Merkel cell carcinoma. Science. 2008; 319:1096–1100. [PubMed: 18202256]

Hall BJ, Pincus LB, Yu SS, et al. Immunohistochemical prognostication of Merkel cell carcinoma: p63 expression but not polyomavirus status correlates with outcome. J Cutan Pathol. 2012; 39:911–917. [PubMed: 22882157]

Harms PW, Patel RM, Verhaegen ME, et al. Distinct gene expression profiles of viral-and nonviral-associated merkel cell carcinoma revealed by transcriptome analysis. J Invest Dermatol. 2013; 133:936–945. [PubMed: 23223137]

Hashida Y, Imajoh M, Nemoto Y, et al. Detection of Merkel cell polyomavirus with a tumour-specific signature in non-small cell lung cancer. Br J Cancer. 2013; 108:629–637. [PubMed: 23322199]

Houben R, Grimm J, Willmes C, et al. Merkel cell carcinoma and Merkel cell polyomavirus: evidence for hit-and-run oncogenesis. J Invest Dermatol. 2012; 132:254–256. [PubMed: 21850029]

Houben R, Shuda M, Weinkam R, et al. Merkel cell polyomavirus-infected Merkel cell carcinoma cells require expression of viral T antigens. J Virol. 2010; 84:7064–7072. [PubMed: 20444890]

Indra AK, Warot X, Brocard J, et al. Temporally-controlled site-specific mutagenesis in the basal layer of the epidermis: comparison of the recombinase activity of the tamoxifen-inducible Cre-ER(T) and Cre-ER(T2) recombinases. Nucleic Acids Res. 1999; 27:4324–4327. [PubMed: 10536138]

Inuzuka H, Shaik S, Onoyama I, et al. SCF(FBW7) regulates cellular apoptosis by targeting MCL1 for ubiquitylation and destruction. Nature. 2011; 471:104–109. [PubMed: 21368833]

Jaeger T, Ring J, Andres C. Histological, immunohistological, and clinical features of merkel cell carcinoma in correlation to merkel cell polyomavirus status. J Skin Cancer. 2012:e983421.

Khalili K, Sariyer IK, Safak M. Small tumor antigen of polyomaviruses: role in viral life cycle and cell transformation. J Cell Physiol. 2008; 215:309–319. [PubMed: 18022798]

Koepp DM, Schaefer LK, Ye X, et al. Phosphorylation-dependent ubiquitination of cyclin E by the SCFFbw7 ubiquitin ligase. Science. 2001; 294:173–177. [PubMed: 11533444]

Kwun HJ, Shuda M, Feng H, et al. Merkel Cell Polyomavirus Small T Antigen Controls Viral Replication and Oncoprotein Expression by Targeting the Cellular Ubiquitin Ligase SCF(Fbw7.). Cell Host Microbe. 2013; 14:125–135. [PubMed: 23954152]

Lemos BD, Storer BE, Iyer JG, et al. Pathologic nodal evaluation improves prognostic accuracy in Merkel cell carcinoma: analysis of 5823 cases as the basis of the first consensus staging system. J Am Acad Dermatol. 2010; 63:751–761. [PubMed: 20646783]

Mao JH, Kim IJ, Wu D, et al. FBXW7 targets mTOR for degradation and cooperates with PTEN in tumor suppression. Science. 2008; 321:1499–1502. [PubMed: 18787170]

Maricich SM, Wellnitz SA, Nelson AM, et al. Merkel cells are essential for light-touch responses. Science. 2009; 324:1580–1582. [PubMed: 19541997]

Morrison KM, Miesegaes GR, Lumpkin EA, et al. Mammalian Merkel cells are descended from the epidermal lineage. Dev Biol. 2009; 336:76–83. [PubMed: 19782676]

Mumby M. PP2A: unveiling a reluctant tumor suppressor. Cell. 2007; 130:21–24. [PubMed: 17632053]

Nateri AS, Riera-Sans L, Da CC, et al. The ubiquitin ligase SCFFbw7 antagonizes apoptotic JNK signaling. Science. 2004; 303:1374–1378. [PubMed: 14739463]

Niller HH, Wolf H, Minarovits J. Viral hit and run-oncogenesis: genetic and epigenetic scenarios. Cancer Lett. 2011; 305:200–217. [PubMed: 20813452]

Pantulu ND, Pallasch CP, Kurz AK, et al. Detection of a novel truncating Merkel cell polyomavirus large T antigen deletion in chronic lymphocytic leukemia cells. Blood. 2010; 116:5280–5284. [PubMed: 20817850]

Ramirez A, Bravo A, Jorcano JL, et al. Sequences 5′ of the bovine keratin 5 gene direct tissue-and cell-type-specific expression of a lacZ gene in the adult and during development. Differentiation. 1994; 58:53–64. [PubMed: 7532601]

Rodriguez-Viciana P, Collins C, Fried M. Polyoma and SV40 proteins differentially regulate PP2A to activate distinct cellular signaling pathways involved in growth control. Proc Natl Acad Sci U S A. 2006; 103:19290–19295. [PubMed: 17158797]

Sablina AA, Hahn WC. SV40 small T antigen and PP2A phosphatase in cell transformation. Cancer Metastasis Rev. 2008; 27:137–146. [PubMed: 18214640]

Schwitalla S, Fingerle AA, Cammareri P, et al. Intestinal tumorigenesis initiated by dedifferentiation and acquisition of stem-cell-like properties. Cell. 2013; 152:25–38. [PubMed: 23273993]

Shuda M, Chang Y, Moore PS. Merkel cell polyomavirus-positive Merkel cell carcinoma requires viral small T-antigen for cell proliferation. J Invest Dermatol. 2014; 134:1479–1481. [PubMed: 24217011]

Shuda M, Feng H, Kwun HJ, et al. T antigen mutations are a human tumor-specific signature for Merkel cell polyomavirus. Proc Natl Acad Sci U S A. 2008; 105:16272–16277. [PubMed: 18812503]

Shuda M, Kwun HJ, Feng H, et al. Human Merkel cell polyomavirus small T antigen is an oncoprotein targeting the 4E-BP1 translation regulator. J Clin Invest. 2011; 121:3623–3634. [PubMed: 21841310]

Sihto H, Kukko H, Koljonen V, et al. Merkel cell polyomavirus infection, large T antigen, retinoblastoma protein and outcome in Merkel cell carcinoma. Clin Cancer Res. 2011; 17:4806–4813. [PubMed: 21642382]

Stetsenko GY, Malekirad J, Paulson KG, et al. p63 Expression in Merkel Cell Carcinoma Predicts Poorer Survival yet May Have Limited Clinical Utility. Am J Clin Pathol. 2013; 140:838–844. [PubMed: 24225752]

Tilling T, Moll I. Which are the cells of origin in merkel cell carcinoma? J Skin Cancer. 2012:e680410.

Van KA, Mascre G, Youseff KK, et al. Epidermal progenitors give rise to Merkel cells during embryonic development and adult homeostasis. J Cell Biol. 2009; 187:91–100. [PubMed: 19786578]

Westermarck J, Hahn WC. Multiple pathways regulated by the tumor suppressor PP2A in transformation. Trends Mol Med. 2008; 14:152–160. [PubMed: 18329957]

Zur Hausen H. Novel human polyomaviruses--re-emergence of a well known virus family as possible human carcinogens. Int J Cancer. 2008; 123:247–250. [PubMed: 18449881]

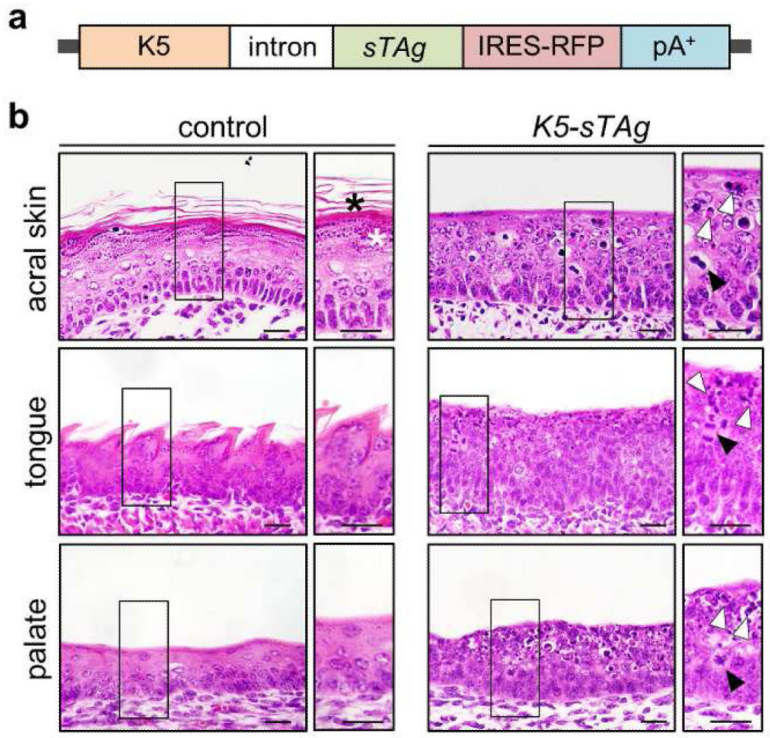

Figure 1. Epithelial transformation in pre-term mouse embryo expressing MCPyV sTAg

A) Transgenic cassette including bovine K5 promoter, wild-type MCPyV sTAg and IRES-tdTomato (RFP), designated *K5-sTAg*. B) Histology of indicated epithelia from pre-term control and *K5-sTAg* embryos. Rectangles indicate regions shown at higher magnification. Note increased thickness of epithelia in *K5-sTAg* mice and loss or reduction of differentiated granular (white asterisk) and cornified (black asterisk) cell layers seen in controls. White arrowheads indicate pyknotic nuclei with condensed chromatin suggestive of apoptosis in *K5-sTAg* epithelia; black arrowheads identify suprabasal mitotic figures, which are normally restricted to basal or immediate suprabasal cell layers. Scale bars = 25 μm.

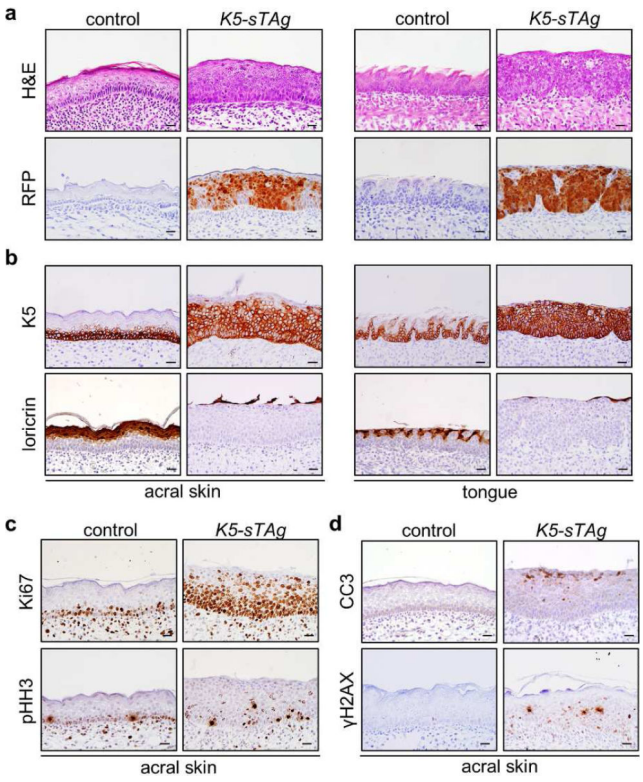

Figure 2. MCPyV sTAg alters epithelial differentiation, proliferation, and apoptosis

A) H&E and RFP immunostaining of acral skin and tongue showing disorganized, hyperplastic epithelia and widespread transgene (RFP) expression. B) Expansion of the basal layer marker K5 and impaired expression of the granular cell marker loricrin in sTAg-expressing epithelia. C) Striking upward expansion of Ki67-expressing proliferating cells and phospho-histone H3 (pHH3)-expressing mitotic cells in sTAg-expressing epidermis. D) Immunostaining for the apoptosis marker CC3 and DNA damage-response marker γH2AX in sTAg epidermis. Scale bars = 25 μm.

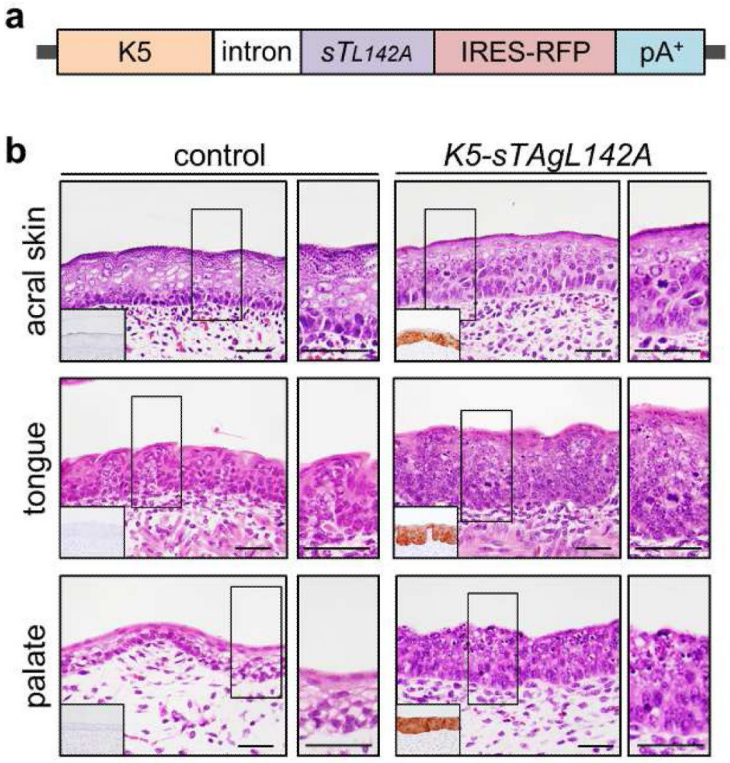

Figure 3. Epithelial transformation by a PP2A binding-deficient sTAg mutant

A) *K5-sTAgL142A* transgene construction identical to *K5-sTAg* in Figure 1A except for L142A substitution which blocks sTAg binding to PP2A. B) H&E and RFP immunostaining in sections from acral skin, tongue, and palate, showing features of transformation similar to those in *K5-sTAg* mice and robust transgene expression. RFP immunostaining is shown in insets. Scale bars = 50 μm.

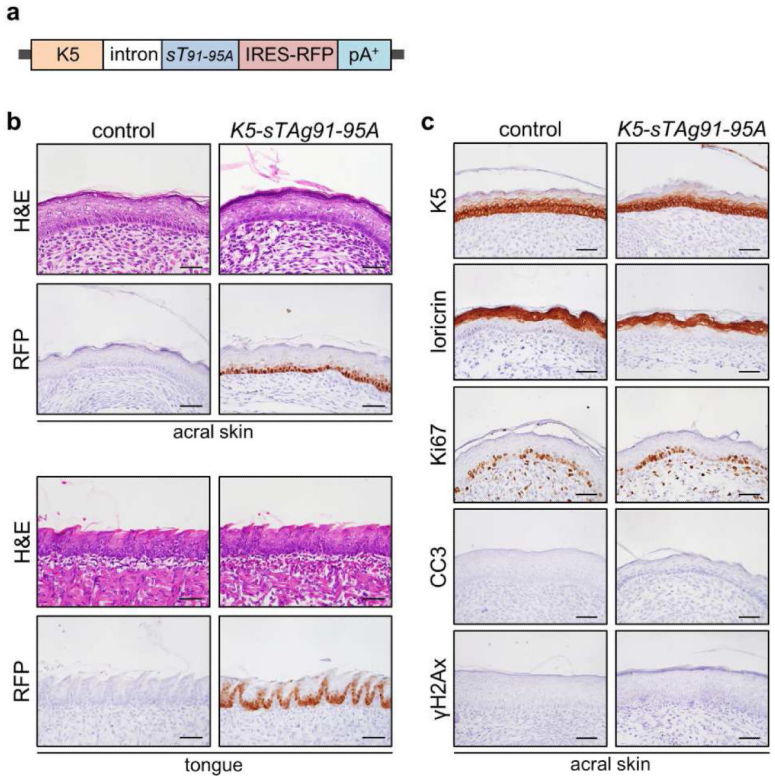

Figure 4. Lack of epithelial transformation by an LTAg stabilization domain (LSD) sTAg mutant

A) Transgene construction identical to *K5-sTAg* in Figure 1A except for 91-95A substitutions which block sTAg binding to Fbxw7. B) Similar histology of acral skin and tongue in sections from control and *K5-sT91-95A* transgenic mice, despite robust RFP expression in basal layer cells of transgenic mice. C) Similar profile of epidermal markers and proliferation, and lack of CC3 and γH2AX immunostaining in control and *K5-sT91-95A* transgenic acral skin. Scale bars = 50 μm.

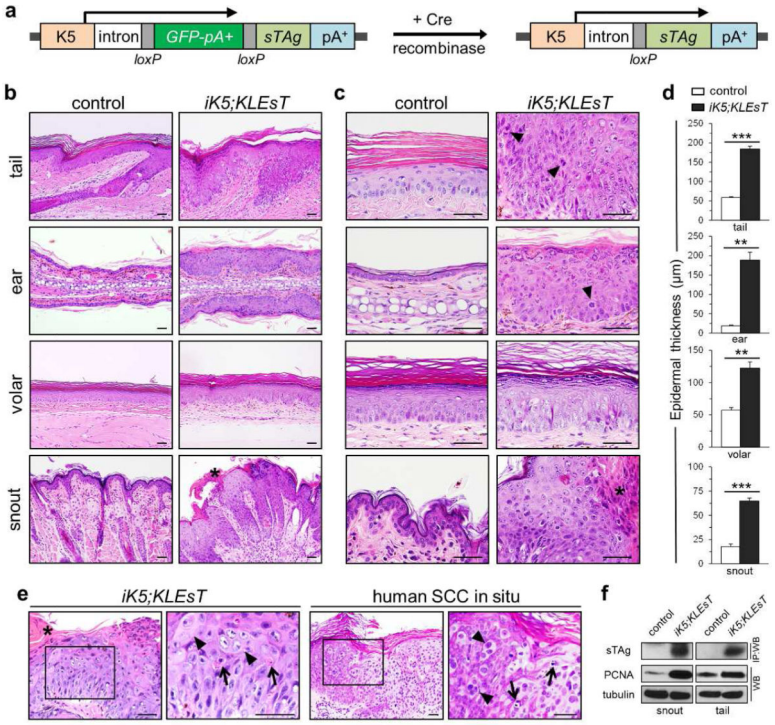

Figure 5. Postnatal activation of sTAg induces epidermal transformation in adult mice

A) Design of *KLEsT* transgene expressing eGFP and dormant sTAg, in which Cre-mediated recombination and GFP excision allow K5-driven sTAg expression. B,C) Phenotype of *K5-CreER;KLEst (iK5;KLEsT)* bitransgenic mice 2-3 weeks post tamoxifen treatment at P21. Note massive epidermal hyperplasia, disorganized stratification, suprabasal mitoses (arrowheads), and hyperkeratotic regions (asterisk). D) Quantification of increased epidermal thickness at indicated sites (N=3 for each column, error bars indicate SEM, **p<0.005, ***p<0.0003). E) Similarity of *iK5;KLEsT* epidermal phenotype and human SCC *in situ*. Both lesions show a severely disorganized epithelium, pale-staining atypical epidermal cells (arrowheads), apoptotic cells (arrows), and hyperkeratosis (asterisk). F) Expression of sTAg in lysates from *iK5;KLEsT* mice collected 11 days (snout) and 21 days (tail) after tamoxifen treatment. sTAg was detected by immunoprecipitation and immunoblotting using 2t2 monoclonal Ab. Scale bars = 50 µm.

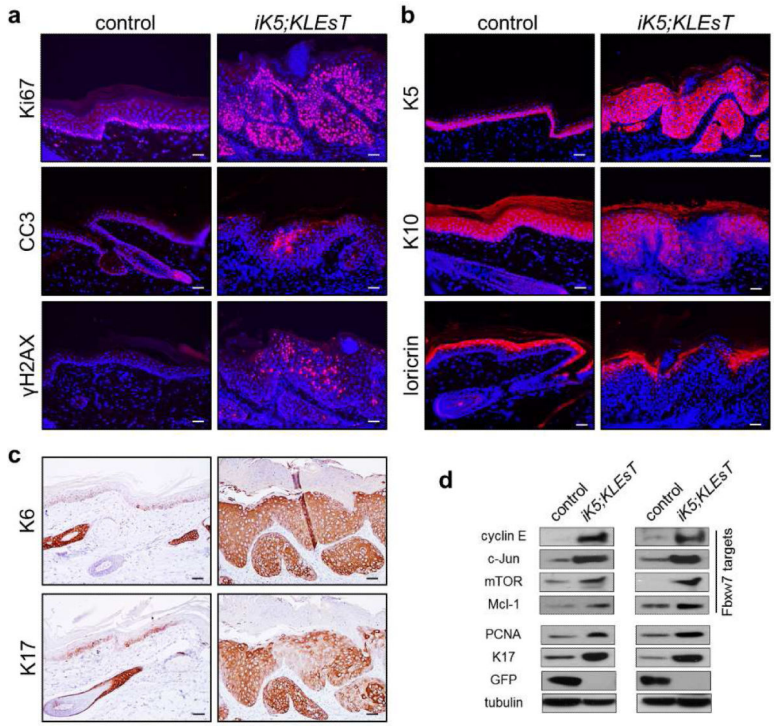

Figure 6. Postnatal activation of sTAg induces markers of epidermal transformation and accumulation of Fbxw7 target proteins

A) Expansion of proliferative cell layers (Ki67), increased apoptosis (CC3), and DNA damage (γH2AX) in tail epidermis of sTAg-expressing *iK5;KLEsT* mice three weeks after treatment with tamoxifen. B) Expansion of cell layers expressing K5 and focal reductions in expression of the differentiation markers K10 and loricrin. C) Upregulation of hyperplasia-associated keratins K6 and K17 in epidermis of *iK5;KLEsT* mice. Normal expression of these keratins is largely restricted to the hair follicle. D) Immunoblotting for Fbwx7 targets, PCNA, K17, and GFP in sets of snout lysates from control and *iK5;KLEsT* mice, collected 24 days (left panels) or 28 days (right panels) after tamoxifen treatment. Loss of GFP expression confirms efficient recombination of the *KLEsT* transgene. Scale bars = 50 μm.